Feedforward Ripple Cancellation for a Full-Bridge Converter

Deron K. Jackson Steven B. Leeb

Abstract—

This paper presents a feedforward ripple cancellation technique for use with a full-bridge DC-DC converter. The full-bridge is used to energize an inductive coupling that serves as an isolating connector in a battery charging system. Feedforward ripple cancellation prevents large ac currents from flowing into the battery terminals in response to unavoidable ac ripple on the inverter input bus voltage. A computationally inexpensive technique for implementing ripple cancellation using either analog or digital hardware is described and demonstrated on a 1500 watt hardware prototype.

I. Background

CONVENTIONAL circuits in the power delivery range from 0 to 10 kW for charging batteries often employ a power-factor correcting utility (PFC) interface. Near-unity power factor operation is essential to ensure maximum power delivery capability and to minimize the generation of harmonic currents. In a two-stage architecture, which additionally provides isolation, a bridge inverter operates from a DC link created by the PFC rectifier [1]. We are engaged in the design and analysis of an inductively coupled, two-stage power conditioning architecture for all sorts of servomechanical drives, including for application as a battery charger. A schematic of a unidirectional (charge only) architecture is shown in Fig. 1. A bidirectional supply with two-way, charge and discharge capability is employed for the experiments in this paper [2].

The full-bridge inverter impresses a high frequency AC signal on the primary of a transformer. The secondary waveform is rectified to provide a DC output voltage for charging. This DC-DC stage provides isolation through an inductive coupling or separable transformer, which is considered by some to maximize operator safety and connector life [1–3]. To minimize dissipation in the separable coupling, a significant concern for a practical connector, the inverter is operated at a fixed frequency and near-unity duty ratio. Control of the charging current is accomplished by actively varying the output voltage of the PFC rectifier.

The power factor correction stage produces a controlled DC output voltage with a small, twice-line frequency, e.g., 120 Hz, ripple component. If the ripple is not eliminated during the second stage DC/DC conversion, it passes directly to the load. The battery load shown in Fig. 1 will typically include filter capacitors to minimize high, switch-frequency voltage ripple. However, it is often not cost effective to provide filtering to eliminate low, near-utility-frequency ripple. The peak-to-peak amplitude of the voltage ripple at the DC bus might be on the order of 1% of its DC value. For a resistive load or loads with a "low-pass" character, e.g., a mechanically loaded servomotor, such a small variation is of little consequence. However, in a battery charging application, the load behaves, at least to a simple approximation, as a voltage source with a relatively small series resistance [4], [5]. This series resistance is generally so small that even a slight voltage ripple will induce significant current ripple into the battery. Depending on the battery technology, this ripple could lead to excessive, unacceptable peak currents, and even discontinous charging current. This paper presents a practical scheme for minimizing the effects of the DC bus voltage ripple without requiring feedback information from the secondary side of the transformer. The ripple cancellation approach is demonstrated with results from a 1500 watt prototype.

II. Converter Topology

A simplified sketch of the full-bridge converter topology is shown in Figure 2. Only the components necessary for unidirectional, forward power flow are illustrated, although the 1500 Watt prototype is capable of bidirectional operation for charging and dis-

The authors are with the Laboratory for Electromagnetic and Electronic Systems, Massachusetts Institute of Technology, Cambridge, MA 02139, USA

0-7803-5864-3/00/$10.00 © 2000 IEEE

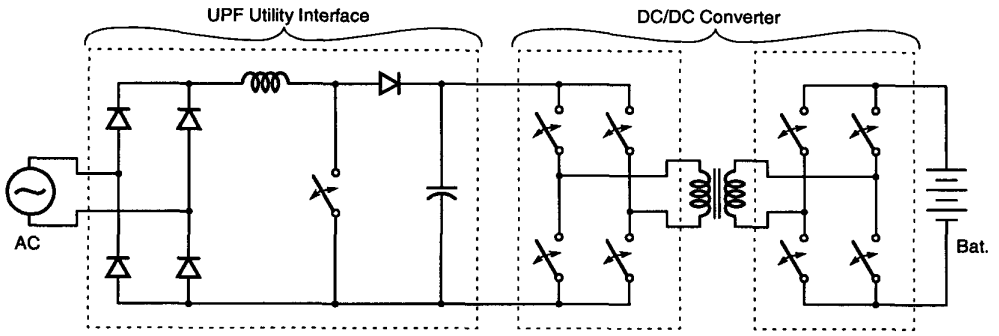

Fig. 1. Circuit topology for an inductively-coupled battery charger (see text).

charging or conditioning operations. MOSFETs Q_1 through Q_4 form a full-bridge inverter. The inverter drives the primary of the inductive coupling through a large DC blocking capacitor C_{bl}. The four switches are gated at a frequency of 100 kHz using a phase-shifted pulse-width modulation pattern [6].

In principle, pulse-width modulation (PWM) control could be used to vary the output voltage from its maximum all the way down to zero. However, the conversion efficiency decreases as the PWM duty ratio is lowered from unity. This decrease is due in part to an increase in the rms switch currents relative to the output current. In the prototype, therefore, duty-ratio control is used only to cancel the 120-Hz small-signal voltage ripple. The nominal duty ratio remains within a few percent of unity. Large signal voltage control is accomplished by varying the PFC bus voltage at the input to the inverter.

Pulse-width modulation of the voltage V_{AB} seen across the primary of the inductive coupling is controlled by adjusting the phase shift between the gate drives applied to each leg of the converter. Zero phase shift yields an effective duty ratio of zero, while a phase shift of π yields a unity-duty ratio. By adjusting the phase shift for PWM control, active ripple cancellation is possible.

III. Feedforward Ripple Cancellation

The steady-state bus voltage at the input to the DC/DC stage can be described as

$$v_{bst}(t) = V_{bst} + r(t) \tag{1}$$

where V_{bst} is the nominal or DC level and $r(t)$ is the 120-Hz ripple component. Under PWM control the output voltage of the DC/DC stage is linearly related to the duty-ratio command by

$$v_o(t) = d(t)Nv_{bst}(t) = d(t)N(V_{bst} + r(t)) \tag{2}$$

where d(t) is the duty ratio and N is the effective transformer turns ratio. Voltage droop caused by the coupling leakage inductance does not affect the ripple cancellation. Therefore, it has been ignored to simplify the discussion. Exact ripple cancellation requires a duty ratio of

$$d(t) = \frac{DV_{bst}}{V_{bst} + r(t)} \tag{3}$$

where D is a constant slightly less than one. As desired, the expression for the steady-state output voltage becomes a constant $v_o(t) = DNV_{bst}$.

The nonlinear expression in (3) would require an expensive analog implementation or a digital solution using a time-varying division. A linear approximation of the expression in (3) can be found by taking the first term in its binomial series expansion, as follows:

$$d(t) = D - \frac{D}{V_{bst}} r(t). \tag{4}$$

This linear approximation is simpler to implement and yields nearly ideal performance. The resulting output voltage is found by substituting (4) into (2):

$$v_o(t) = DNV_{bst} - \frac{DN}{V_{bst}} r(t)^2 \tag{5}$$

Although the expression in (5) is not a constant, the relative amplitude of the AC component is greatly reduced. Significant reduction in the AC

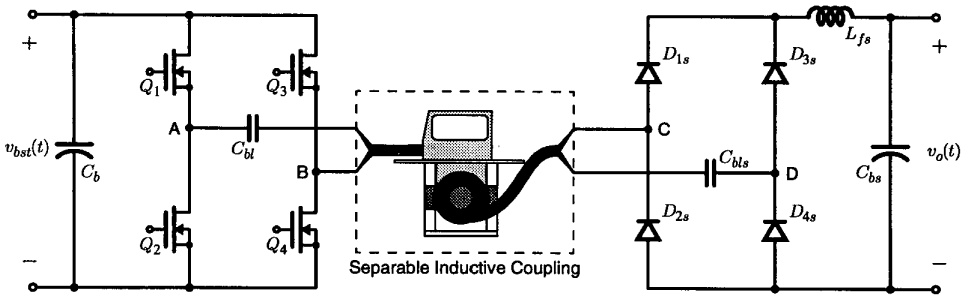

Fig. 2. Simplified schematic of the full-bridge prototype.

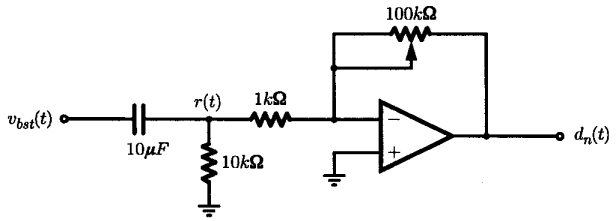

Fig. 3. Ripple extraction filter.

component requires only that V_{bst} is much greater than the amplitude of $r(t)$, and this condition is automatically satisfied by a well-designed PFC stage. Thus, if the amplitude of the input voltage ripple is 1%, the output ripple amplitude should be reduced by over 99%. The amplitude of the remaining ripple is insignificant.

In practice, one approach to implement the feedforward cancellation scheme is as follows. A first-order analog high-pass filter, with a corner frequency of approximately 18 Hz (sufficiently below 120 Hz to avoid affecting $r(t)$), is used to separate $r(t)$ from a measurement of $v_{bst}(t)$. The filter employed in our experimental prototype is shown in Fig. 3. The measured ripple component $r(t)$ is scaled by D/V_{bst}, yielding the intermediate variable $d_n(t)$. The variable $d_n(t)$ is then subtracted from a constant duty-ratio command D using an op-amp subtractor, yielding $d(t)$. The required perturbation $d_n(t)$ is small, so D is selected as close to unity as possible to ensure that there is little or no conduction loss penalty from the freewheeling current in the DC/DC stage. Obviously, this calculation can also be easily implemented on a microcontroller if available.

IV. Experimental Results

Figures 4 and 5 schematically illustrate a complete bidirectional full-bridge topology. Since active ripple cancellation was only desired during battery charging, the topology was designed to provide PWM control only during forward power flow. During reverse power flow, the duty ratio is fixed at unity.

A. Prototype Hardware

Figure 4 shows the configuration for forward power flow. In this mode MOSFETs Q_1 through Q_4 are active while Q_{1s} through Q_{4s} are held off, leaving the anti-parallel diodes to perform rectification. In the prototype, fast HFA3QPA6QC diodes are employed in an anti-parallel configuration with IRFP450 MOSFETS to provide better overall performance than that yielded by the MOSFETS with their internal body diodes. The C_p capacitances shown explicitly in Figs. 4 and 5 are in fact the parasitic capacitances associated with the MOSFETS and diodes. The relay S_s is opened so that an output LC (inductor-capacitor) filter is formed by L_{fs} and C_{bs}. A filter inductor L_{fs} is required for PWM operation because, when the duty ratio is less than unity, The inductor L_{fs} supports the voltage difference between the transformer secondary and the output. Along with this filter inductor comes an unwanted ringing between L_{fs} and the rectifier capacitances. This ring is lossy, and it typically increases the total DC/DC conversion losses by about 20% [7]. In addition, the ring increases the voltage stress on the secondary-side rectifiers. An external clamp circuit may be added if necessary.

The configuration for reverse power flow is shown in Fig. 5. In this case the roles of the switches are re-

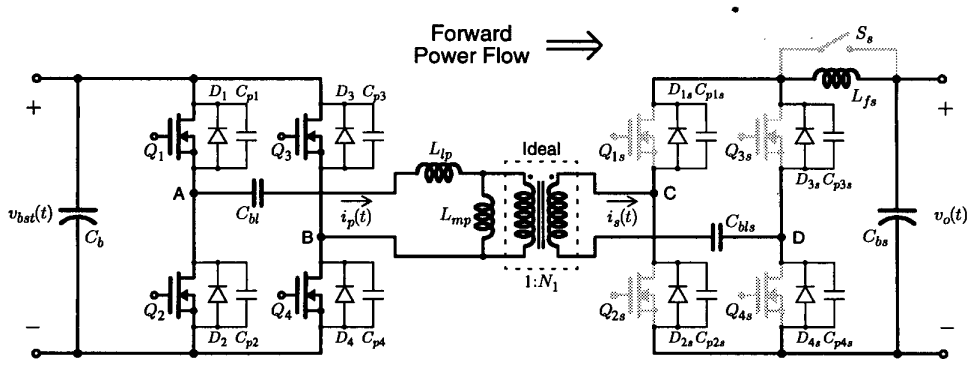

Fig. 4. Full-bridge converter FORWARD operation

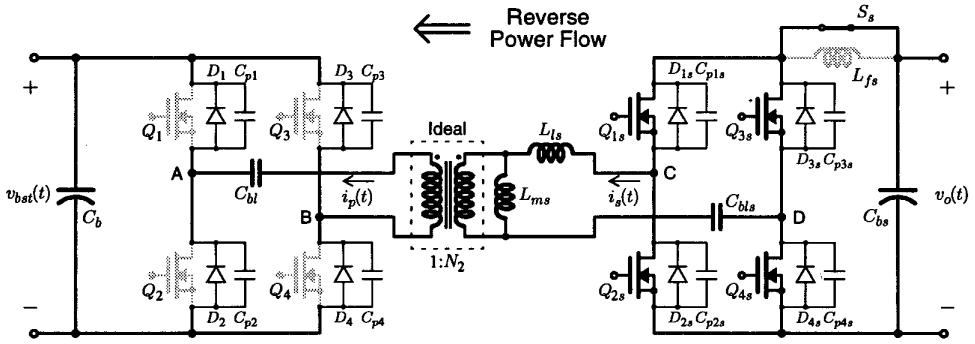

Fig. 5. Full-bridge converter REVERSE operation

versed. MOSFETs Q_{1s} through Q_{4s} are active, while Q_1 through Q_4 are held off. The relay S_s is closed so that v_o, which is now the "input" voltage to the full bridge, forms a stiff bus voltage for Q_{1s} through Q_{4s}. No output filter inductor (analogous to L_{fs}) is required – unity duty-ratio operation is possible with a capacitor-only filter. Thus, there is no lossy ring, and the energy in the parasitic rectifier capacitances is transferred to the load. In the prototype, a bidirectional UPF interface is employed to return power from the load to the utility; details of this arrangment may be found in [2].

Phase-shifted PWM operation provides zero-voltage switching. This reduces switching losses by permitting full recovery of the energy in the MOSFET parasitic capacitances. Provided the leakage inductance, magnetizing inductance, and parasitic capacitances are sized appropriately, ZVS can be guaranteed over a wide operating range. Zero-voltage switching operation of the full bridge is reviewed in [6] and [7]. A Unitrode UC3875 PWM controller chip operates the MOSFETS in the prototype in the phase-shifted PWM pattern. This chip accepts a duty-cycle input voltage waveform and operates the full-bridge to ensure that the commanded duty cycle is provided through appropriate timing of the switch firings and relative phase. To provide active ripple cancellation, the duty-cycle command waveform in the prototype is computed using analog computation as outlined in the previous section.

Experimental waveforms from the prototype full-bridge converter are plotted in Fig. 6. The six traces on the left show waveforms recorded during FORWARD operation at a power level of approximately 900 W from a DC bus voltage of approximately 310 V. The voltage waveforms v_A and v_B demonstrate the ZVS transitions. The phase shift between v_A and v_B is very near to π as indicated by the approximately 95% duty ratio of primary voltage v_{AB}. Small perturbations in this duty ratio can be used to cancel the ripple in v_{bst}. The bottom two traces at the left of Fig. 6 show the voltage and current measured at

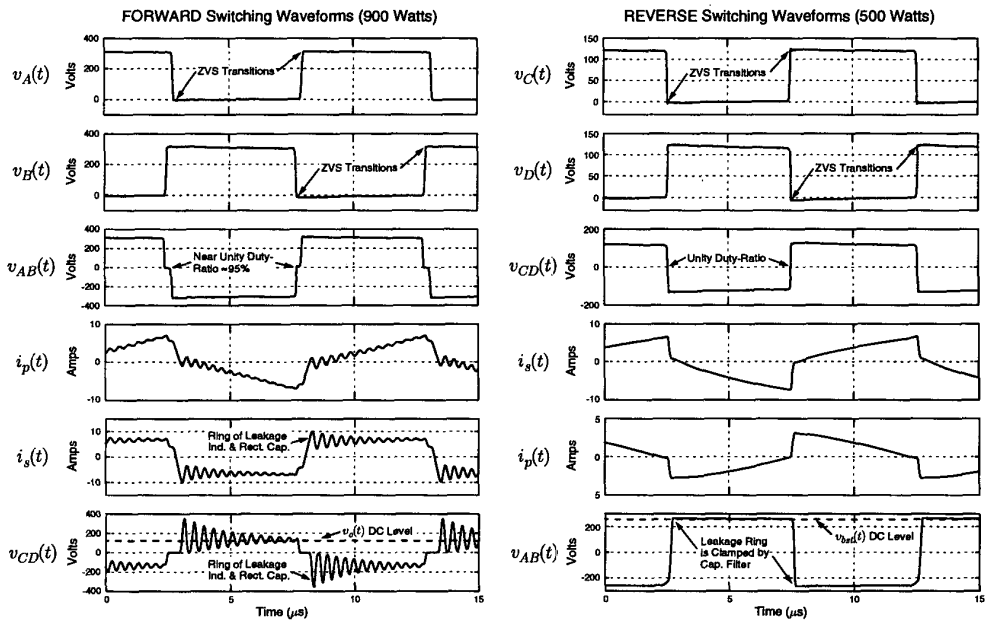

Fig. 6. Experimental switching waveforms for FORWARD and REVERSE operation

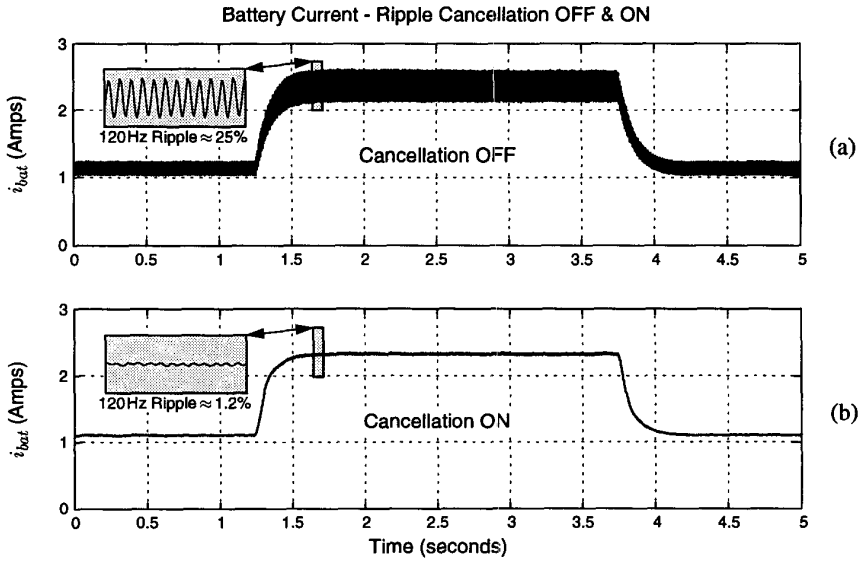

Fig. 7. Experimental waveforms showing the effect of ripple cancellation.

the input to the secondary-side rectifier. The waveforms clearly show the expected oscillatory ring of the leakage inductance and the parasitic rectifier capacitances.

The six traces on the right of Fig. 6 show experimental waveforms during REVERSE operation at a power level of approximately 500 W from a DC battery voltage of approximately 120 V. In this case the inductive coupling is driven from the secondary side at 100 kHz with unity duty ratio. Zero-voltage switching is illustrated by the waveforms v_C and v_D. Since reverse operation occurs at unity duty ratio, an output filter inductor is unnecessary. As a result, the voltage v_{AB}, shown at the bottom right in the figure, is effectively clamped by the filter capacitor C_b.

B. Active Ripple Cancellation

This need for active ripple cancellation is exemplified by the experimental waveforms in Fig. 7. The experimental data in the top trace was recorded using the prototype hardware with the ripple cancellation circuitry disabled. The waveforms show a 25% (peak-to-peak) current ripple while charging a 120-V lead-acid battery pack with a nominal charging current of 2.3 A. The corresponding voltage ripple during this experiment is approximately 0.5% (peak-to-peak). Although the voltage ripple is relatively small, the current ripple is significant. As the nominal charge current is increased, the current ripple can easily exceed 100%, resulting in a discontinuous battery current.

Experimental waveforms demonstrating the effectiveness of the ripple cancellation technique are shown in Fig. 7. The expanded views demonstrate a measured reduction in current ripple from 25% to 1.2%. Also, note that the transient step changes in the output current have essentially no affect on the ripple cancellation. The remaining ripple in Fig. 7 can be attributed to the linear approximation of the optimum $d(t)$ and to a slight phase shift from the filtered measurement of $r(t)$, which is used to generate the feedforward command.

V. Discussion

Discontinuous or high-ripple charging current may increase the temperature and pressure of a battery during charge. Future battery chemistries and high-rate charge profiles may require that such ripple is eliminated. The PWM voltage control capability of the phase-shifted full-bridge DC/DC converter makes it possible to provide active ripple cancellation. The prototype full-bridge converter uses a feedforward control technique to accomplish this.

We expect that this cancellation technique could be extended to half-bridge configurations using the asymmetrical half-bridge control technique, discussed in [8]. However, with this control approach, the output voltage is non-linearly related to the switch duty ratio. Hence, the ripple cancellation might be more complicated to implement in the half-bridge configuration.

Acknowledgements

This research was funded by AMP, Incorporated, MIT's Carl Richard Soderberg Career Development Chair, and a National Science Foundation CAREER award. The authors gratefully acknowledge the valuable advice and support of Joseph Sweeney, James Wise, Dr. Howard Peiffer, and Bob Grebe. Essential hardware for this project was made available through generous donations from the Intel Corporation, Tektronix, and Hewlett-Packard.

References

[1] K.W. Klontz, A. Esser, P.J. Wolfs, and D.M. Divan, "Converter Selection for Electric Vehicle Charger Systems with a High-Frequency High-Power Link," *Power Electronics Specialists Conference,* June, 1993, pp. 855-861.

[2] D. Jackson, "Inductively Coupled Power Transfer for Electromechanical Systems," *Ph.D. Thesis,* Massachusetts Institute of Technology, May, 1998.

[3] Society of Automotive Engineering, *SAE J-1773 Electric Vehicle Inductive Coupling Recommended Practice,* Warrendale, PA, February 1995.

[4] D. Linden, *Handbook of Batteries - Second Edition,* McGraw-Hill, Inc., New York, NY, 1995.

[5] D.Temkin, M. McVey and U. Carlsson, "A Spacecraft Electrical Battery Simulator," *Intersociety Energy Conversion Engineering Conference,* August, 1990, pp. 19-26.

[6] Unitrode Integrated Circuits, "Phase-Shifted, Zero Voltage Transition Design Considerations and the UC3875 PWM Controller," Application Note U-136, 1993.

[7] L. Mweene, "The Design of Front-End DC-DC Converters of Distributed Power Supply Systems with Improved Efficiency and Stability," Ph.D. Thesis, Massachusetts Institute of Technology, September 1992.

[8] P. Imbertson and N. Mohan, "Asymmetrical Duty Cycle Permits Zero Switching Loss in PWM Circuits with No Conduction Loss Penalty," *IEEE Transactions on Industry Applications,* Vol. 29, No. 1, Jun./Feb. 1993, pp. 121-125.